Atomic short-range order and spin-glass behaviour in concentrated Cu-Mn alloys

1990 J. Phys.: Condens. Matter 2 6593

(http://iopscience.iop.org/0953-8984/2/31/012)

J. Phys.: Condens. Matter 2 (1990) 6593–6601. Printed in the UK

Atomic short-range order and spin-glass behaviour in concentrated Cu–Mn alloys

R Clad†, R Kuentzler† and W Pfeiler‡

† IPCMS, Unité Mixte 380046, CNRS, Institut de Physique, 3 rue de l'Université, F-67084 Strasbourg, France

‡ Institut für Festkörperphysik, Universität Wien, Strudlhofgasse 4, A-1090 Vienna, Austria

Received 9 February 1990

Abstract. The effect of atomic short-range order (SRO) in **Cu**–Mn (5–30 at.% Mn) on the spin-glass properties is studied by measuring the magnetic behaviour and the low-temperature specific heat for two well defined equilibrium states of SRO. Usual spin-glass features are observed. The freezing temperature T_f as well as the coefficient γ^* of the linear specific heat term appear to be not sensitive to SRO, whereas the amplitude of the peak susceptibility at T_f is drastically increased. The results are compared with previous work after different thermal treatments.

1. Introduction

Atomic short-range order (SRO), which means local deviations from a random distribution over the lattice positions of the different kinds of atom, seems to be a common property of concentrated solid solutions. In alloys with a magnetic component the spatial distribution of the magnetic atoms in the non-magnetic host which is frozen in to low temperatures may be of crucial importance for the magnetic interactions at the spin-glass temperature. It therefore is essential to know how the magnetic properties at low temperatures are correlated with well defined states of SRO frozen in from high temperatures.

As an archetype for a spin glass, **Cu**–Mn has been studied extensively in recent years. However, only a few studies illustrate the interplay between local order and magnetism. Even in the interesting studies of Morgownik and Mydosh [1, 2] and Gibbs *et al* [3] the results on the magnetic behaviour may not be correlated to a certain equilibrium state of SRO owing to a rather inadequate temperature treatment of the samples [4].

It is the aim of the present paper to present results of magnetisation and low-temperature specific heat on **Cu**–Mn samples (5, 8, 13, 16, 20 and 30 at.% Mn) corresponding to two different but definite states of SRO: one state corresponds to the well established SRO state at 200 °C, and the other to the state at 400 °C (350 °C for Cu–13 at.% Mn), which corresponds to a lower degree of SRO.

The main question which should be answered in this way is: how do the above physical quantities vary as a function of concentration with respect to the degree of SRO

0953-8984/90/316593 + 09 $03.50

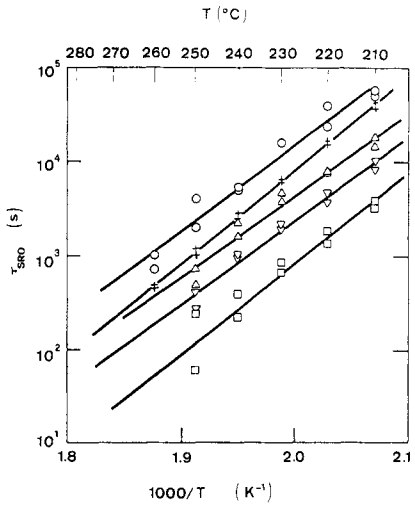

Figure 1. SRO relaxation time as a function of reciprocal temperature of Cu–5 at.% Mn (○), Cu–8 at.% Mn (△), Cu–13 at.% Mn (□), Cu–16 at.% Mn (▽) and Cu–20 at.% Mn (+).

and is there agreement with previous investigations [1–3]? Preliminary results have already been published in [15].

2. Atomic short-range order

The existence of SRO in **Cu**–Mn alloys is well established since the early measurements of Kussmann and Wollenberger [5] and essentially of Scheil and co-workers [6, 7] on magnetic susceptibility and specific heat in **Cu**–Mn alloys with up to 25 at.% Mn. Scheil and co-workers also performed isothermal anneals between 200 and 400 °C.

In recent years, several neutron scattering experiments confirmed the existence of well established SRO [1, 2, 8, 9]. From scattering experiments using polarised and unpolarised neutrons, magnetic SRO was concluded to exist as well as atomic SRO in **Cu**–Mn alloys with up to 50 at.% Mn. From some experimental results, SRO parameters were determined [10–12], which describe the atomic SRO quantitatively by means of a deviation from a random atomic distribution in the different coordination spheres.

Besides neutron scattering experiments, measurements of electrical resistivity after an adequate temperature treatment may give interesting insight into the physics of SRO. The kinetics of SRO adjustment after a small disturbance can be studied with great accuracy, yielding especially the correlation between atomic mobility and degree of SRO. We have detailed this approach in a recent paper [13].

In the present investigation we use results from resistivity measurements on several **Cu**–Mn alloys [14] to select carefully an adequate temperature treatment in order to establish two microstructure states in the **Cu**–Mn alloys investigated, which correspond to certain different but well defined temperatures as equilibrium states; this means states of different but well defined degrees of SRO. For experimental details see [14].

In figure 1 the SRO relaxation times for the adjustment of equilibrium states of SRO is plotted as a function of reciprocal temperature (Arrhenius plot). From this plot we decided to use the following temperature treatment: homogenisation at 750 °C for about 2 h, furnace cooling to 200 °C and annealing at this temperature for more than 50 h

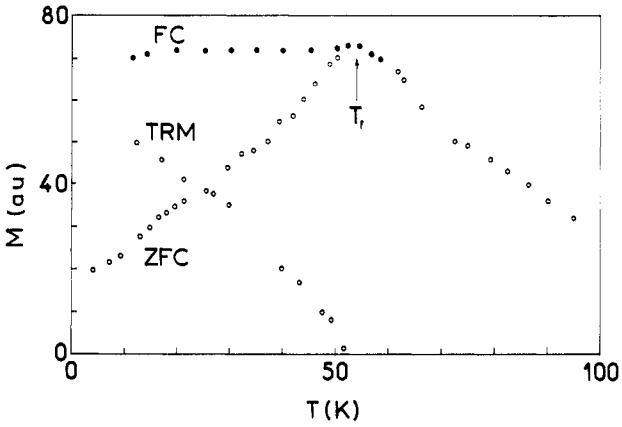

Figure 2. Magnetic susceptibility of Cu–13 at.% Mn annealed at 200 °C: T_f, freezing temperature; ZFC, zero-field-cooled susceptibility; FC, field-cooled susceptibility; TRM, thermoremanent moment.

followed by a water quench. This procedure should yield a well established SRO state corresponding to 200 °C. Because of the low atomic mobility at lower temperatures, an annealing treatment at 100 °C is not suited to achieving an equilibrium structure of SRO within a few months. After measuring the magnetisation and low-temperature specific heat for the samples in this 'ordered' state, the samples were annealed for about 1 h at 400 °C and water quenched. This procedure should yield the 'less ordered' state corresponding to 400 °C. From figure 1 it can be seen that owing to the relation between the quenching rate and atomic mobility a temperature of 400 °C is near to the highest quenching temperature where it should still be possible to freeze in the high-temperature state under the present experimental conditions. For the sample with 13 at.% Mn this temperature treatment was done at 350 °C because of the rather high atomic mobility (short SRO relaxation time) of this material.

3. Magnetic behaviour

The magnetisation measurements were carried out by the induction method. In this method the magnetisation Σ of an ellipsoidal sample is obtained from the integrated voltage–time pulses induced in a system of two detection coils in series. When the sample is displaced from one detection coil to the other in a constant applied field H_a, which is generated by a superconducting solenoid, the output voltage V of the device becomes proportional to the magnetisation Σ of the sample: $V = K\Sigma$. The constant K is determined by calibration with a polycrystalline ellipsoidal standard sample of nickel ($\sigma = \Sigma/m \simeq 58.5$ emu g^{-1} in a field $H_a \geqslant 10$ kOe). The sensitivity of the device is about 10^{-4} emu cgs; the temperature range extends from 1.6 to 300 K.

In figure 2 as an example of the magnetic behaviour of a sample with well established SRO the magnetic susceptibility χ of Cu–13 at.% Mn annealed at 200 °C is shown as a function of temperature; the typical feature of a spin glass is observed. The data were obtained using just one measuring field of 55 Oe. The thermoremanent moment (TRM) is plotted as a moment per field, giving the same units as the susceptibility. A pronounced peak in the zero-field-cooled susceptibility is observed at the freezing temperature T_f, where the TRM disappears. Below T_f the field-cooled susceptibility remains more or less constant and a TRM appears.

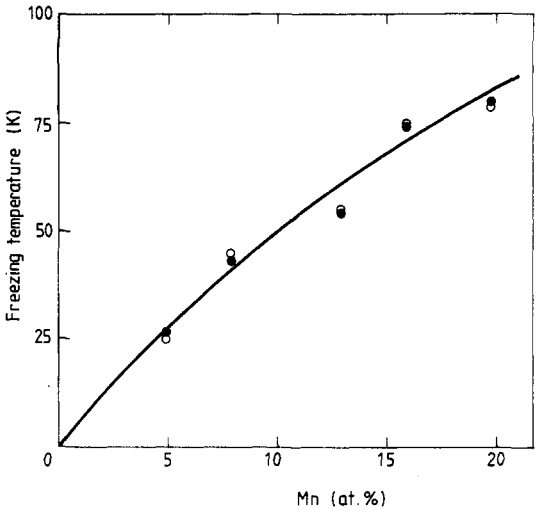

Figure 3. Dependence of freezing temperature on Mn content: ●, 200 °C state; ○, 400 °C state.

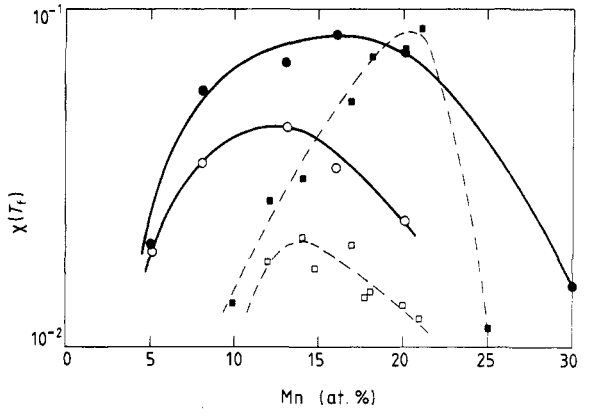

Figure 4. Variation in the peak susceptibility at T_f (in SI units) with Mn concentration on a logarithmic scale: ●, 200 °C state; ○, 400 °C state; ■, annealed for 5 weeks at 100 °C [3]; □, quenched from 850 °C [3].

Figure 3 gives the freezing temperature as a function of Mn content for the samples heat treated in both ways explained earlier. It is observed that, in both cases, T_f increases with increasing concentration not linearly but as c^n with $n < 1$ [16].

The differences in the degree of SRO due to the different thermal treatments applied give no marked change in the freezing temperature for any concentration investigated. This is in some contrast with the results of Gibbs *et al* [3], who observed a slight shift of T_f to higher temperatures with a maximum ΔT of 13 K at about 20 at.% Mn.

In contrast with the spin-freezing temperature a great influence of the thermal treatment on the measured value of susceptibility is observed: a higher degree of SRO is accompanied by a higher value of susceptibility. This is shown in figure 4 (full and open circles with full curves through them), where the peak susceptibilities at T_f for the 200 °C and 400 °C states respectively, are plotted as a function of Mn concentration. These findings correspond to the results of Gibbs *et al* [3] on quenched and aged samples, which are given in figure 4 (open and full squares with broken curves through them) for

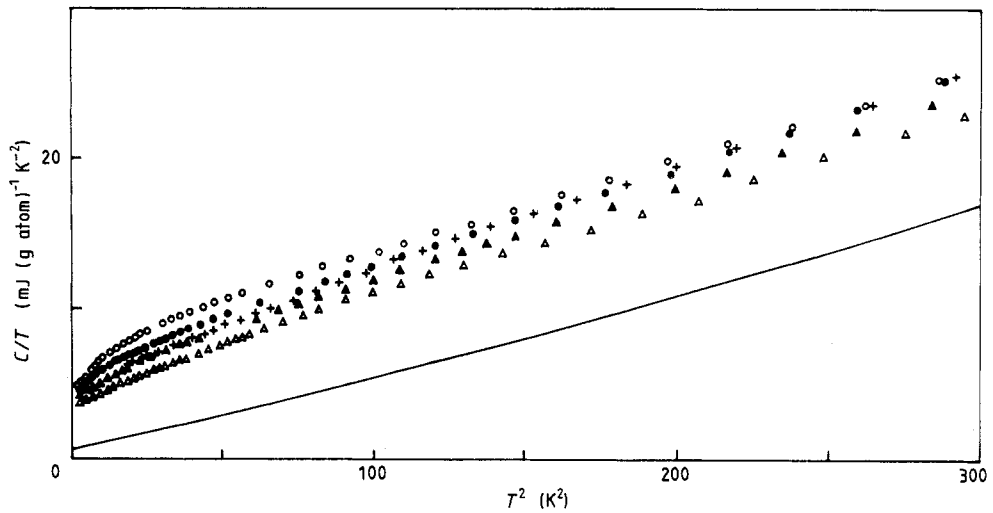

Figure 5. Low-temperature specific heat C/T versus T^2 for Cu–Mn alloys with 5 at.% Mn (○), 8 at.% Mn (●), 13 at.% Mn (▲), 16 at.% Mn (+) and 20 at.% Mn (△).

comparison. There is also a very good agreement with results of AC susceptibility measurements by Pinkvos *et al* [17] on Cu–6 at.% Mn after quenching from various temperatures. On the other hand, figure 4 shows some differences between the present investigation and that of [3]: the shapes of the curves are different and the maxima of the present curves are slightly shifted by about 5 at.% to lower Mn contents.

4. Low-temperature specific heat

The specific heat measurements were performed automatically by a quasi-adiabatic method in the temperature range 1.5–40 K. The temperature is determined with a Cryocal germanium resistor. An accuracy of better than 1% is achieved for metallic materials of about 1 g mass.

The study of low-temperature specific heat between 1.5 and 17 K yields great similarity for all concentrations investigated and no dependence on thermal treatments when C/T is plotted versus T^2 (figure 5); a drastic change is observed in comparison with pure copper (straight line). This corresponds well to previous work by Zimmermann and Hoare [18]. Moreover the magnetic specific heat C_{magn} ($C_{magn} = C_{alloy} - C_{Cu}$) in the investigated temperature range for Cu–5 and Cu–8 at.% Mn shows no indication of a discontinuity or a broad anomaly caused by a cooperative-type ordering, which would be expected at the freezing temperature, where the low-field susceptibility of the same samples displays the well defined cusp. This has already been shown for low Mn concentrations by Wenger and Keesom [19].

Figure 6 shows the linear coefficient γ^* for the behaviour of the specific heat at low temperatures as a function of Mn content. The drastic increase in γ^* up to 5 at.% Mn is followed by a slight decrease. Apart from a small reduction in γ^* (about 5% for the sample with 5 at.% Mn) of the samples in the 400 °C state, no influence of the thermal treatment is observed.

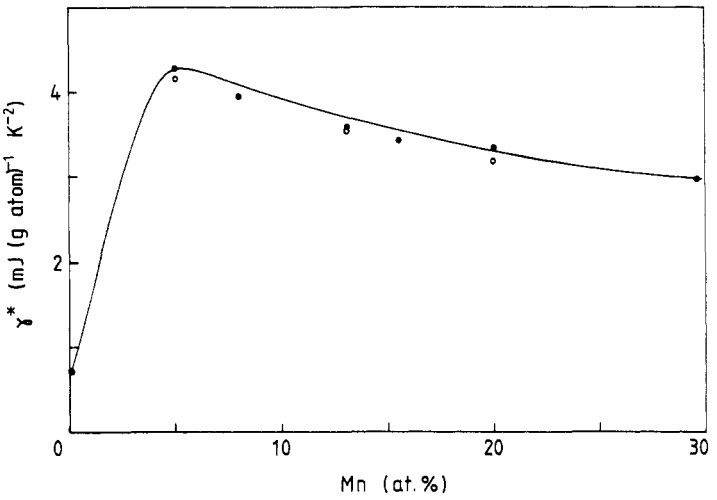

Figure 6. Coefficient γ^* of the linear specific heat term as a function of Mn content: ●, 200 °C state; ○, 400 °C state.

5. Discussion

Well known spin-glass features result for our Cu–Mn samples for both equilibrium states of SRO which were set by the thermal pre-treatment. Surprisingly, the freezing temperature T_f, which increases with increasing concentration, does not seem to be influenced by SRO. Further, the coefficient γ^* of the linear specific heat, which includes magnetic contributions, is only changed a little. However, the amplitude of the susceptibility peak at T_f is drastically affected by SRO since it is enhanced by a factor of up to 3 (Cu–20 at.% Mn). This magnetic behaviour of our samples with definite SRO equilibrium states is similar to what has been observed earlier [3] after quenching from 850 °C and annealing for a long time at 100 °C, respectively, and after quenching from various temperatures [17].

On the other hand, marked differences from [3] are observed with respect to the shape of the curves and the position of the maximum value of the peak susceptibility at T_f. Considering that the results in [3] after quenching may correspond to a temperature of 500 °C (see later) as equilibrium values the low values of $\chi(T_f)$ in this case seem quite reasonable. Yet there remains the difficulty of explaining the rather sharp maximum at 20 at.% Mn of the samples aged at 100 °C in [3]. A consistent interpretation can be given if one assumes that the thermal treatment at temperatures as high as 850 °C due to the high vapour pressure of Mn leads to a loss of Mn content. A degree of evaporation of Mn at 850 °C of about 10^{-5} g cm^{-2} s^{-1} [20] for a 1 h anneal may give a loss of Mn of about 0.04 g, leading to a reduction of about 4 at.% Mn. This way the sharp maximum of the annealed curve in [3] may fall into the region of increased atomic mobility (broken curves in figure 7). Samples in this concentration range during annealing for a long time at 100 °C come closer to the equilibrium state than samples with other concentrations (compare figure 1) leading to the rather sharp peak.

As shown in figure 4 the influence of SRO on the spin-glass properties essentially enters the peak susceptibility at the spin-glass temperature $\chi(T_f)$. It therefore may be interesting to plot the difference between $\chi(T_f)$ for the high and low degrees of SRO as a

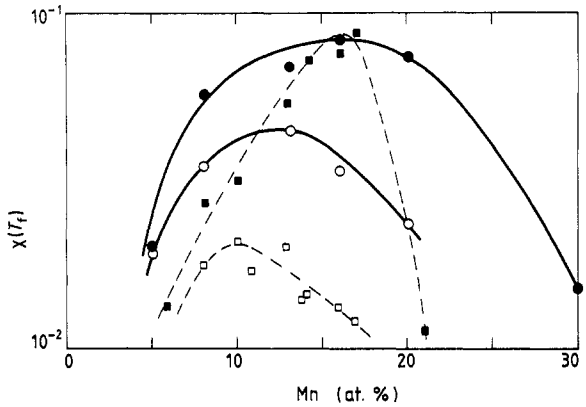

Figure 7. Variation in peak susceptibility at T_f (in SI units) with Mn concentration. Figure 4 is replotted here, but the values from [3] are shifted by about 4 at.% to lower Mn concentrations (– – –).

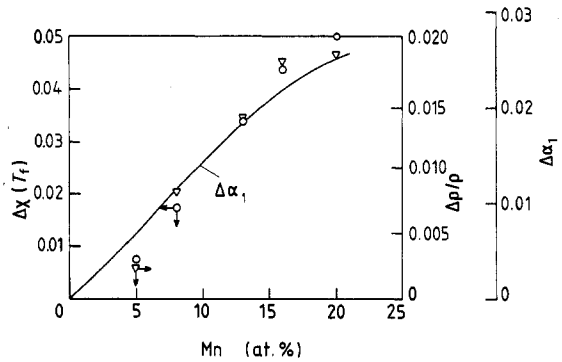

Figure 8. Influence of SRO on magnetic susceptibility (200 and 400 °C) (○) and residual resistivity (200 and 300 °C) (▽) versus Mn content (SI units). This influence is plotted as a difference between a more ordered state and a less ordered state. The differences in the first SRO parameter (200 and 400 °C) as calculated by a cluster variation method [21] are given for a comparison (full curve).

function of Mn content and to compare the values of susceptibility with SRO-induced changes in electrical resistivity [14, 21] and corresponding differences in the SRO parameter as calculated by a nearest-neighbour cluster variation method [21]. It is observed from figure 8 that the variation with Mn concentration of differences in the susceptibility at T_f (corresponding to $\Delta T = 200\,°C$) and differences in resistivity (corresponding to $\Delta T = 100\,°C$) are very similar, and both are in good accordance with calculated differences in the SRO parameter.

To estimate the influence of the temperature treatment on the results observed in [3], $\chi_{max}(T_f)$ is plotted as a function of temperature in figure 9. Owing to the appropriate heat treatment the present results can be considered to correspond to the temperatures of 200 and 400 °C as equilibrium states of SRO. The assumption of a linear relation between $\chi_{max}(T_f)$ and the corresponding temperature (equilibrium line), which may be

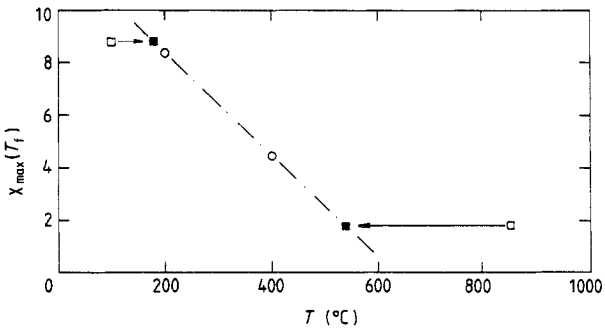

Figure 9. Maximum values of peak susceptibility (SI units) as a function of temperature. The present values at 200 and 400 °C generate a sort of 'equilibrium line'. From this, the effective state of the samples in [3] can be estimated by shifting the values of $\chi_{max}(T_f)$ (□) horizontally to the 'equilibrium line' (■). Annealing for 5 weeks at 100 °C corresponds to about 180 °C, and the quench from 850 °C corresponds to about 550 °C.

justified by the similar dependence on SRO of susceptibility and resistivity (figure 8), indeed yields the reasonable values of about 180 °C (annealing for 5 weeks at 100 °C) and 550 °C (quenched from 850 °C) as the corresponding temperatures for the samples used in [3].

It is planned to extend the present study using the same conditions to other archetypal spin glasses (**Au**–Fe, **Au**–Mn and **Pt**–Mn), for which a greater influence of SRO on the magnetic behaviour is to be expected [2].

Acknowledgment

The work was financially supported by the Austrian 'Fonds zur Förderung der wissenschaftlichen Forschung' under grant 5894.

References

[1] Morgownik A F and Mydosh J A 1981 *Phys. Rev.* B **24** 5277
[2] Morgownik A F and Mydosh J A 1983 *Solid State Commun.* **47** 325
[3] Gibbs P, Harders T M and Smith J H 1985 *J. Phys. F: Met. Phys.* **15** 213
[4] Pfeiler W and Reihsner R 1985 *J. Phys. F: Met. Phys.* **15** 2547
[5] Kussmann A and Wollenberger H J 1956 *Z. Naturwiss.* **43** 395
[6] Scheil E and Wachtel E 1957 *Z. Metallk.* **48** 571
[7] Scheil E and Norman W 1960 *Z. Metallk.* **51** 165
[8] Wells P and Smith H J 1971 *J. Phys. F: Met. Phys.* **1** 763
[9] Hirabayashi M, Koiwa M, Yamaguchi S and Kamata K 1978 *J. Phys. Soc. Japan* **45** 1591
[10] Davis J R, Burke S K and Rainford B D 1980 *J. Magn. Magn. Mater.* **15–8** 151
[11] Cable J W, Werner SA, Felcher GP and Wakabayashi N 1984 *Phys. Rev.* B **29** 1268
[12] Harders T M, Hicks T J and Smith J H 1983 *J. Phys. F: Met. Phys.* **13** 1262
[13] Pfeiler W 1988 *Acta Metall.* **36** 2417
[14] Reihsner R and Pfeiler W 1985 *J. Phys. Chem. Solids* **46** 1431
[15] Clad R, Kuentzler R and Pfeiler W 1988 *J. Physique Coll.* **49** C8 109
[16] Cannella V 1973 *Amorphous Magnetism* ed H O Hooper and A M de Graaf (New York: Plenum) p 195
[17] Pinkvos H, Gygax F N, Lippelt E, Neuhaus R, Schenck A, Schwink Ch and van der Wal A J 1986 *J. Magn. Magn. Mater.* **54–7** 119

[18] Zimmerman J E and Hoare F E 1960 *J. Phys. Chem. Solids* **17** 52
[19] Wenger L E and Keesom P H 1976 *Phys. Rev.* B **13** 4053
[20] Espe W 1959 *Werkstoffkunde der Hochvakuumtechnik* vol 1 (Berlin: Volkseigener Betrieb Deutscher Verlag der Wissenschaften) p 882
[21] Pfeiler W and Reihsner R 1986 *Phys. Status Solidi* a **97** 377